Acta Crystallographica Section F
Structural Biology and Crystallization Communications
ISSN 1744-3091

Crystallization and preliminary crystallographic analysis of *Gibberella zeae* extracellular lipase

Yuna Sun,[a,b]‡ Ming Li,[c]‡ Yan Zhang,[a,b] Lifang Liu,[c] Ye Liu,[c] Zheng Liu,[c] Xumei Li[a,b] and Zhiyong Lou[b]*

[a]National Laboratory of Macromolecules, Institute of Biophysics, Chinese Academy of Science, Beijing 100101, People's Republic of China, [b]Tsinghua–Nankai–IBP Joint Research Group for Structural Biology, Tsinghua University, Beijing 100084, People's Republic of China, and [c]Novozymes (China) Investment Co. Ltd China Headquarters, 14 Xinli Road, Shangdi Zone, Haidian District, Beijing 100085, People's Republic of China

‡ These authors contributed equally to this work.

Correspondence e-mail: louzy@xtal.tsinghua.edu.cn

Received 27 February 2008
Accepted 25 June 2008

Fusarium head blight, one of the most destructive crop diseases, is mainly caused by *Fusarium graminearum* (known in its sexual stage as *Gibberella zeae*). *F. graminearum* secretes various extracellular enzymes that have been hypothesized to be involved in host infection. One of the extracellular enzymes secreted by this organism is the *G. zeae* extracellular lipase (GZEL), which is encoded by the *FGL1* gene. In order to solve the crystal structure of GZEL and to gain a better understanding of the biological functions of the protein and of possible inhibitory mechanisms of lipase inhibitors, recombinant GZEL was crystallized at 291 K using PEG 3350 as a precipitant. A data set was collected to 2.8 Å resolution from a single flash-cooled crystal (100 K). The crystal belonged to space group $P2_12_12_1$, with unit-cell parameters $a = 78.4$, $b = 91.0$, $c = 195.8$ Å, $\alpha = \beta = \gamma = 90^\circ$. The presence of four molecules was assumed per asymmetric unit, which gave a Matthews coefficient of 2.6 Å^3 Da^{-1}.

1. Introduction

Fusarium head blight (FHB), which is one of the most destructive and economically important crop diseases, is mainly caused by the phytopathogenic fungus *Fusarium graminearum* (known in its sexual stage as *Gibberella zeae*). *F. graminearum* produces a variety of mycotoxins that potentially pose serious threats to human health and animal production. FHB has recently spread worldwide owing to the increase in global temperature, resulting in great economic loss. FHB is a devastating disease of wheat and barley and is a growing threat to the worldwide food supply (Bai & Shaner, 2004). Ascospores of *G. zeae* released from perithecia are usually the major primary inoculum in disease epidemics (Bai & Shaner, 2004). During infection, fungal pathogens secrete various extracellular enzymes that have been reported to be involved in host infection. One such extracellular enzyme secreted by *G. zeae* is an extracellular lipase (GZEL) encoded by the *FGL1* gene.

Lipases (triacylglycerol acylhydrolases; EC 3.1.1.3) catalyze the hydrolysis of long-chain triglycerides into fatty acids and glycerol. Lipases are ubiquitous and are widely distributed in different organisms. They are also important biocatalysts and have broad biotechnological applications in the detergent, food-production and pharmaceutical industries (Jaeger & Reetz, 1998). Moreover, lipases have become candidates for the virulence factors of pathogenic bacterial strains and fungal species (Nasser Eddine *et al.*, 2001). For example, addition of antibodies to the extracellular lipase secreted by *Botrytis cinerea* was found to suppress lesion formation on tomato leaves *in vitro* (Nasser Eddine *et al.*, 2001; Commenil *et al.*, 1995).

The GZEL lipase has been demonstrated to act as a virulence factor and is important to the pathogenicity of *F. graminearum* (*G. zeae*; Voigt *et al.*, 2005). It has been suggested that inhibition of the lipase by ebelactone B (a known lipase inhibitor) might reduce the severity of the disease (Voigt *et al.*, 2005).

The crystal structures of GZEL homologues, such as the lipases from *Thermomyces* (*Humicola*) *lanuginosa*, *Aspergillus niger* and

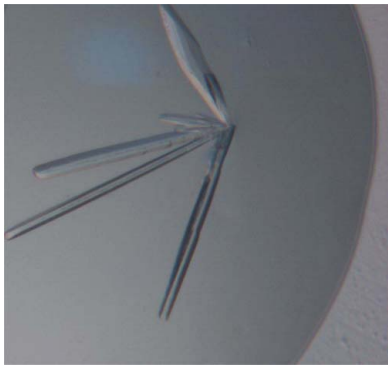

Rhizopus niveus (Brzozowski *et al.*, 2000; McAuley *et al.*, 2004; Derewenda *et al.*, 1994; Kohno *et al.*, 1996), offer hints about the catalytic mechanism of GZEL. However, GZEL may have features that are distinct from these other lipases as its sequence contains a unique C-terminal extension. In the present study, we have PCR-amplified and cloned the *FGL1* gene. We report the crystallization and preliminary crystallographic studies of GZEL. The structure of this protein will improve our understanding of its catalytic mechanism and explain how GZEL is inhibited by lipase inhibitors.

2. Materials and methods

2.1. Protein expression and purification

The entire coding sequence of FGL1 was amplified from *F. graminearum* cDNA by polymerase chain reaction. Two individual PCR fragments were obtained by using two sets of primer pairs independently: Na (5′-GATCCACCATGCGTCTCCTGTCACTCC-TC-3′) and Cb (5′-CTGATGAGCGGCTGGCGTGAG-3′), and Nb (5′-CACCATGCGTCTCCTGTCACTCCTC-3′) and Ca (5′-AATTC-TGATGAGCGGCTGGCGTGAG-3′). The two fragments were mixed with equal amounts of DNA. After a process of denaturing and renaturing, *Bam*HI and *Eco*RI restriction sites were generated at the 5′-end and the 3′-end, respectively. The fragment was then ligated to the expression vector pLIZG7 with the same restriction digestions. A EFHHHHHHP tag was fused to the C-terminus of the recombinant protein. A transformation into ElectroMax DH10B competent cells (Invitrogen) by electroporation was performed. Transformed cells were plated on LB plates containing 100 µ*M* ampicillin. After overnight incubation at 310 K, a positive clone was selected by colony PCR and confirmed by sequencing. The plasmid DNA of the positive clone was linearized with *Pme*I (NEB) and transformed into *Pichia pastoris* KM71 (Invitrogen) following the manufacturer's instructions. Transformants were grown on a histidine-deficient MD plate for 2–3 d. Four positive candidates were inoculated into 3 ml BMSY and shaken at 301 K for 3 d until the OD_{600} reached 20. Methanol was then added to the culture daily to a final concentration of 0.5% for the following 4 d.

On day 4 of induction, the cultures were harvested by centrifugation. The activity of the supernatant was tested on olive oil/Bright Green plates at pH 7.0 (Niu *et al.*, 2008). The positive-candidate clones showed dark green zones around the holes. Positive supernatants also showed a protein band of the appropriate size on SDS–PAGE with Coomassie staining.

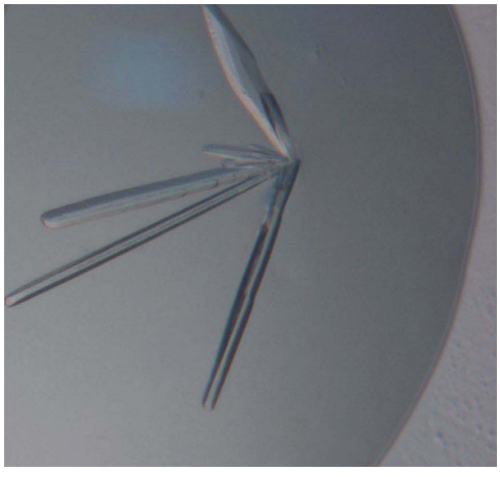

Figure 1
Typical crystal of GZEL.

Table 1
Data-collection and processing statistics.

Values in parentheses are for the highest resolution shell.

Space group	$P2_12_12_1$
Unit-cell parameters (Å, °)	a = 78.4, b = 91.0, c = 195.8, $\alpha = \beta = \gamma = 90$
Wavelength (Å)	1.5418
Resolution range (Å)	50.0–2.8 (2.9–2.8)
Total reflections	326163 (25352)
Unique reflections	34080 (3169)
Average $I/\sigma(I)$	9.6 (8.0)
$R_{\rm merge}$† (%)	10.1 (48.0)
Data completeness (%)	97.7 (92.3)

† $R_{\rm merge} = \sum_{hkl}\sum_i |I_i(hkl) - \langle I(hkl)\rangle| / \sum_{hkl}\sum_i I_i(hkl)$, where $\langle I(hkl)\rangle$ is the mean intensity of the observations $I_i(hkl)$ of reflection hkl.

The culture supernatant was separated from the cells by centrifugation and the pH of the supernatant was adjusted to 7.0. The supernatant was then filtered and applied onto Ni-Sepharose FF equilibrated with 25 m*M* Tris–HCl pH 7.0 plus 0.3 *M* NaCl. The target protein was eluted with an imidazole gradient from 0 to 1 *M*. Fractions from the column were analyzed for activity. Fractions with enzyme activity were pooled and concentrated. The samples were then loaded onto a Superdex 75 gel-filtration column equilibrated with 25 m*M* Tris–HCl pH 8.0 plus 0.15 *M* NaCl. The eluted active lipase was concentrated and dialyzed against 25 m*M* Tris–HCl pH 8.0. The lipase was checked by SDS–PAGE and the pure fractions were prepared for crystallization trials.

2.2. Crystallization

The freshly prepared protein was concentrated to 10 mg ml^{-1} in 5 m*M* Tris pH 8.0. Crystallization was performed by the hanging-drop vapour-diffusion method in 24-well plates at 291 K. Initial crystallization conditions were screened using Hampton Research Crystal Screen kits. 1 µl protein solution was mixed with 1 µl reservoir solution and equilibrated against 200 µl reservoir solution. Small crystals were found in various conditions within 3 d. Many of the crystals grew as hollow sticks and had poor diffraction quality. Fine-shaped and good-quality crystals were selected from a condition consisting of 0.2 *M* ammonium sulfate, 0.1 *M* bis-tris pH 5.5, 25%(*w*/*v*) PEG 3350 (Fig. 1). These crystals grew to final dimensions of about 50 × 50 × 200 µm within 4 d and belonged to space group $P2_12_12_1$.

2.3. Data collection and processing

A 2.8 Å resolution diffraction data set was collected from a single GZEL crystal at 100 K using an in-house Rigaku MM-007 generator and a MAR345dtb detector. The beam was focused using Osmic mirrors. Crystals were immersed in cryoprotectant for 5–10 s, picked up with a nylon loop and flash-cooled in a stream of nitrogen gas cooled to 100 K. The cryoprotectant was prepared by adding 25%(*v*/*v*) glycerol to the mother-liquor reservoir. A total of 360 frames of data were collected (Fig. 2). Processing of the diffraction images and scaling of the integrated intensities were performed using the *HKL*-2000 software package (Otwinowski & Minor, 1997).

3. Results and discussion

Initially, GZEL crystals were obtained in many conditions from the screening kits but showed poor X-ray diffraction. Many of the crystals grew as hollow sticks. Optimization was performed and improved

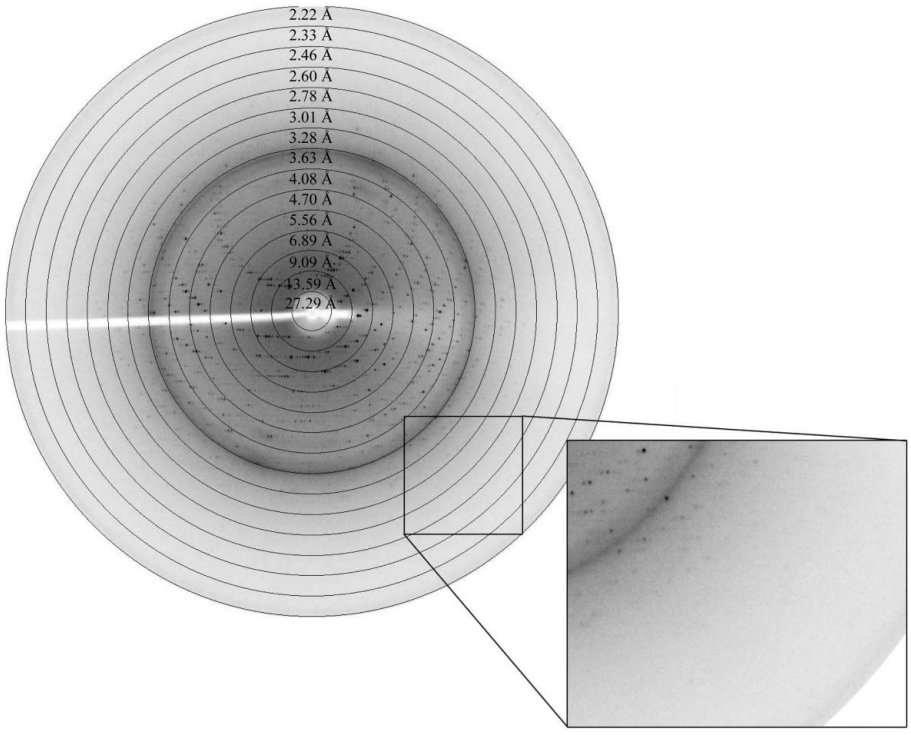

Figure 2
A typical diffraction pattern of GZEL crystals. The exposure time was 300 s, the crystal-to-detector distance was 150 mm and the oscillation range per frame was 1°. The diffraction image was collected on a MAR345 image-plate detector. An enlarged image is shown on the right.

crystals were obtained using the following reservoir solution: 0.2 *M* ammonium sulfate, 0.1 *M* bis-tris pH 5.5, 25%(*w*/*v*) PEG 3350. The crystals grown using this optimized condition diffracted to 2.8 Å resolution and a data set was subsequently collected from a single crystal (Fig. 1). The crystals belonged to space group $P2_12_12_1$, with unit-cell parameters a = 78.4, b = 91.0, c = 195.8 Å. We assumed the presence of four molecules per asymmetric unit, which gave a Matthews coefficient of 2.6 $Å^3$ Da^{-1} and a solvent content of 48% (Matthews, 1968). Complete data-collection statistics are given in Table 1.

Initial molecular replacement was performed using the crystal structure of *Thermomyces* (*Humicola*) *lanuginosa* lipase excluding the bound substrate (Brzozowski *et al.*, 2000) as a model. This protein (PDB code 1ein) has over 40% identity to GEZL but is 32 residues shorter. Molecular replacement was first performed using *CNS* v.1.2 (Brünger *et al.*, 1998), but no clear solution was found in the rotation and translation functions. An alternative approach using *Phaser* (McCoy *et al.*, 2005) was then performed. A clear solution was found with rotation-function *Z*-score and translation-function *Z*-score values of 5.5 and 6.3, respectively. *DM* (Cowtan, 1994) was then used to improve the quality of the electron-density map. The *R* factor is still over 40% and structure refinement is under way.

We are grateful to Novozymes (China) for providing the GZEL plasmid and thank Professor Zihe Rao for generous support. This work was supported by the '973' Project (grant No. 2006CB806503) and the NSFC (grant No. 30221003).

References

Bai, G. & Shaner, G. (2004). *Annu. Rev. Phytopathol.* **42**, 135–161.
Brünger, A. T., Adams, P. D., Clore, G. M., DeLano, W. L., Gros, P., Grosse-Kunstleve, R. W., Jiang, J.-S., Kuszewski, J., Nilges, M., Pannu, N. S., Read, R. J., Rice, L. M., Simonson, T. & Warren, G. L. (1998). *Acta Cryst.* D**54**, 905–921.
Brzozowski, A., Savage, H., Verma, C., Turkenburg, J., Lawson, D. & Patkar, S. (2000). *Biochemistry*, **39**, 15071–15082.
Commenil, P., Belingheri, L., Sancholle, M. & Dehorter, B. (1995). *Lipids*, **30**, 351–356.
Cowtan, K. (1994). *Jnt CCP4/ESF–EACBM Newsl. Protein Crystallogr.* **31**, 34–38.
Derewenda, U., Swenson, L., Green, R., Wei, Y., Dodson, G. G., Yamaguchi, S., Haas, M. J. & Derewenda, Z. S. (1994). *Nature Struct. Biol.* **1**, 36–47.
Jaeger, K. E. & Reetz, M. T. (1998). *Trends Biotechnol.* **16**, 396–403.
Kohno, M., Funatsu, J., Mikami, B., Kugimiya, W., Matsuo, T. & Morita, Y. (1996). *J. Biochem. (Tokyo)*, **120**, 505–510.
McAuley, K. E., Svendsen, A., Patkar, S. A. & Wilson, K. S. (2004). *Acta Cryst.* D**60**, 878–887.
McCoy, A. J., Grosse-Kunstleve, R. W., Storoni, L. C. & Read, R. J. (2005). *Acta Cryst.* D**61**, 458–464.
Matthews, B. W. (1968). *J. Mol. Biol.* **33**, 491–497.
Nasser Eddine, A., Hannemann, F. & Schafer, W. (2001). *Mol. Genet. Genomics*, **265**, 215–224.
Niu, X., Liu, Y., Knötzel, J. C. F. & Munk, S. (2008). Patent WO/2008/006781.
Otwinowski, Z. & Minor, W. (1997). *Methods Enzymol.* **276**, 307–326.
Voigt, C. A., Schafer, W. & Salomon, S. (2005). *Plant J.* **42**, 364–375.